Interpreting fractional anisotropy in gliomas: correlation with 1H spectroscopy and consideration of SNR

F. A. Howe[1], T. R. Barrick[2], G. A. Fellows[3], and A. J. Wright[4]

[1]Cardiac & Vascular Sciences, St George's, University of London, London, United Kingdom, [2]Clinical Neuroscience, St George's, University of London, London, United Kingdom, [3]Academic Neurosurgery, St George's, University of London, London, [4]Radiology, UMC st. Radboud University Hospital, Nijmegen, Netherlands

Introduction: Diffusion tensor imaging (DTI) may enable delineation of infiltrative brain tumours such as gliomas more accurately than conventional MRI[1]. Objective criteria for defining the DTI characteristics (e.g. FA and MD) that relate to infiltration would enable maps of likely tumour infiltration to be created using statistical analysis techniques. It has been recently shown that independent component analysis of ^{1}H spectra from MRSI data of gliomas can define regions related to tumour core, infiltration and normal brain with specific DTI characteristics[2], indicating that metabolic information from MRSI data may aid image segmentation when combined with DTI. NAA and FA are independent metrics that are expected to decrease with tumour infiltration and loss of neuronal structure but a mixed tissue model is needed to describe the characteristics of each voxel. Since FA is calculated from principal diffusion magnitude images, for a purely isotropic medium there is a non-zero estimated FA due to noise[3] biasing the data. Here we investigate the FA and NAA distribution in glioblastomas and consider the effect of SNR on the measurement of low FA values.

Methods: ***Data acquisition*** 10 patients with histopathologically diagnosed glioblastoma multiforme were studied prior to treatment. MRI/MRS was performed at 1.5T (SIGNA, GE Milwaukee) and included: 2D MRSI with 16 by 16 phase encode steps over 22 cm FOV and 15 mm slice thickness using PRESS with TE 30ms & TR 2000ms; DTI with b = 1000 s mm^{-2} and 12 gradient orientations[2]; T2 and FLAIR images. ***Data reconstruction*** The raw MRSI data was zero-filled once in both spatial dimensions to give a nominal voxel size of 7 x 7 x 15 mm^3 and LCModel was used for metabolite quantification. Fractional anisotropy (FA) and median diffusivity (MD) maps were co-registered to the MRSI data and average FA and MD calculated for each spectroscopy voxel[2]. ***Simulation of NAA v. FA distributions*** were obtained using a three compartment model with 700 random samples constrained by W+T+N=1, where W=white matter, T=tumour and N=necrosis represent the tissue fractions in each voxel. For each sample (i.e. a voxel measurement) NAA and FA was calculated from the tissue fraction weighted sum with values taken from normal distributions generated for each tissue type: white matter NAA = 2 ± 0.2 a.u., FA= 0.4 ± 0.1; and parameters for tumour and necrosis treated as variables to be determined. An ***FA minimum*** (***FA$_{noise}$***) due to magnitude noise was estimated calculating an isotropic diffusion weighted signal in each gradient orientation for an MD of 0.001 mm^2 s^{-1} with added Gaussian noise for a SNR range of 19 to 46 dB. The mean and standard deviation of calculated FA was then determined from 2000 samples using analytical expressions for the diffusion tensor matrix[4,5].

Results: A scatter plot of NAA concentration against FA created from all 10 GBM datasets showed a trend for FA to decrease with NAA as expected, but with an intercept of non-zero FA for voxels with zero NAA (Fig. 1). Histogram analysis show that with increasing NAA there was a monotonic decrease in voxel numbers; FA had a more Gaussian distribution but skewed towards lower FA values. The image data had a measured SNR range of 34 to 46 dB with a typical tumour MD of 0.001 mm^2 s^{-1}. The simulated FA$_{noise}$ was normally distributed and was 0.5 ± 0.15 at SNR 19dB, decreasing to 0.1 ± 0.03 at 34dB, 0.05 ± 0.015 at 40dB and 0.02 ± 0.007 at 46dB. Assuming that the measured FA in tumour and necrosis was represented by FA$_{noise}$, then at a medium SNR of 40dB a simulated NAA *v.* FA distribution was calculated as shown in Fig. 2 with an intercept at a value of approximately FA$_{noise}$. Using the FA$_{noise}$ for higher or lower SNR resulted in similar plots as Fig. 2 but shifted to the left and right respectively. By simulating NAA *v.* FA distributions with larger mean and standard deviations for the tumour than FA$_{noise}$ scatter plots similar to Fig. 3 were obtained. The NAA histogram was similar to that of real data in all cases. The FA histogram was highly skewed towards low values if tumour FA was set to FA$_{noise}$, and similar to actual data if a higher range of tumour FA values was used.

Fig 1. Data from 10 GBM patients

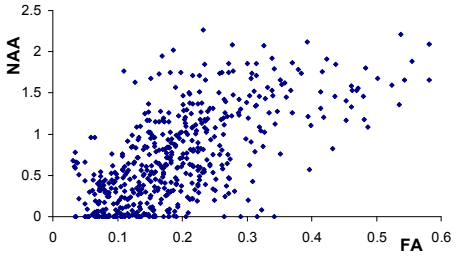

Fig. 2 Simulation: SNR 100, tumour FA = 0.05 ±0.015

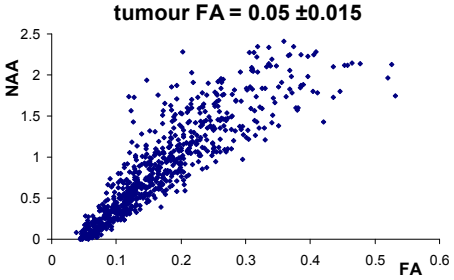

Fig. 3 Simulation: SNR 100, tumour FA = 0.2 ± 0.1

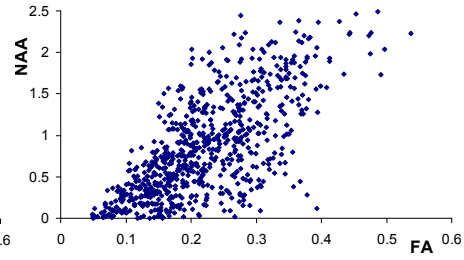

Discussion: Our data provides evidence for diffusion anisotropy in glioblastomas in the absence of functional neurones. Since gliomas have an infiltrative growth pattern the non-zero FA observed at zero NAA may be the result of an anisotropic structure remaining after neuronal loss. By analysing a scatter plot of all data including tumour core, infiltration and necrosis, no assumptions have been made on tissue type except that the intercept at zero NAA should indicate an average FA within a glioblastoma in the absence of neurones without partial volume effects. Simulation of MRSI and DTI data with voxels of mixed tissue was used to demonstrate that the FA offset is most likely due to tumour tissue with non-zero anisotropy and not an offset due to the effects of the magnitude of noise on FA calculation at low FA values. If there is non-zero FA in some purely tumour tissue, then this must be taken into consideration when developing DTI methods to distinguish tumour and white matter tracts. Diffusion-weighted acquisition sequences with higher SNR should improve the ability to distinguish tumour FA from FA$_{noise}$.

References

1. SJ Price et al *Eur Radiol* **17**:1675-84;2007 2. AJ Wright et al. *Magn Reson Med* Epub Sept 25;2009. 3. BA Landmann et al. *NeuroImage* **36**:1123–1138;2007. 4. PJ Basser et al. *Magn Reson Med* **39:**928-934;1998. 5. G Kindlmann et al. *Medical Image Analysis* **11**:492–502;2007.

Acknowledgements

We are grateful to European Union Framework 6 project “eTUMOUR”, grant number LSHC-CT-2004-503094, for support of this work.